AD

WVT-6837

THE OXIDATION MECHANISM OF NICKEL SILICON ALLOY

TECHNICAL REPORT

BY

FUMIHIKO SAEGUSA

DECEMBER 1968

BENÉT LABORATORIES

U.S. ARMY WEAPONS COMMAND

WATERVLIET ARSENAL

WATERVLIET—NEW YORK

AMCMS No. 5025.11.29400

DA Project No. 1-C-0-24401-A328

THE OXIDATION MECHANISM OF NICKEL SILICON ALLOY

ABSTRACT

Thermogravimetric techniques have been used to study oxidation of nickel alloys containing 0.1 to 3.2 wt % silicon at temperatures up to 1300°C. Due to the appearance of internal oxidation the effect of silicon addition on the oxidation process was complex. The thermograms showed a simple curve for lower silicon content, but two consecutive curves for higher content. The oxidation mechanism was interpreted in terms of isothermal kinetics and the corresponding structural changes.

Cross-Reference Data

Oxidation

Corrosion

Nickel

Silicon

Nickel alloys

TABLE OF CONTENTS

FIGURES

TABLES

ACKNOWLEDGEMENT

The author wishes to thank J. F. Cox for his critical review of the manuscript and R. Peterson and R. Lazzaro for their assistance with the experimental work.

INTRODUCTION

It is generally known that the thermal oxidation kinetics of nickel is described by a parabolic rate law over a wide range of temperature with a formation of a single phase oxide, NiO, indicating the reaction is diffusion controlled. Silicon oxidation was recently re-examined[1] [2] and a relationship of mixed parabolic rate was derived based on a model relative to the reactions taking place at the two boundaries of the oxide layer and the diffusion process involved.

Silicon is often used to improve the oxidation resistance of many metals at high temperatures. However, little work has been reported on the oxidation behavior of nickel silicon alloys. In an earlier work, Horn[3] made a qualitative statement indicating that the effect of an addition of a second element on nickel oxidation is greater, the larger the difference in atomic radius. At 900°C the addition of silicon up to 0.5 atm % increases the oxidation rate but further addition up to 4 % reduces the oxidation rate. Gil'dengorn and Rogel'berg[4] studied the oxidation of nickel alloys containing 0.9 - 6.4 wt % silicon in air. It was found that the silicon addition increases the oxidation resistance of nickel at 1000 - 1200°C, and in most cases the oxidation kinetics follow an approximately parabolic rate law particularly at 1100 and 1200°C.

In the present work, a thermogravimetric method was used to study the oxidation of homogeneous nickel silicon alloys in the

temperature range 300 - 1300°C. Thermograms were interpreted in terms of kinetics involving external and internal oxidation. Analyses of structural change were made relative to the corresponding kinetics.

EXPERIMENTAL

Materials: The alloys were prepared from high-purity materials in an arc-melter. Zone-refined nickel with the following analysis: Ag < 0.02; Al 0.3; Fe 12; Si 0.2 ppm and 6/9s silicon were used. The bars were cold worked to 1/8 inch thickness and annealed in vacuum. Analysis of the alloys for silicon gave the following composition in weight %: 0.08, 0.50, 1.00, 2.98, and 3.21. One-quarter inch square coupon specimens weighing approximately 1 gram were cut from the sheets. Thc surfaces were polished through 100 grit emery paper and degreased prior to use. Chemically pure oxygen supplied from a cylinder was further improved by successive passage through a purifier and dryer train. The oxygen flow rate was maintained at 100 cm^3/min throughout the runs.

Apparatus: Mettler's thermoanalyzer was used for gravimetric measurements. The specimen was supported in a fine platinum wire basket positioned over the top of a thermocouple tip to minimize the difference in temperature reading. Weight changes were continuously recorded as the specimen was heated at a linear heating rate or at a constant temperature in a steady flow of oxygen. For the linearly-programmed-temperature experiments, the heating rate was

4°C/min, while the temperature was controlled within ± 0.5°C. The weight recording sensitivity was 0.1 mg.

After oxidation, the oxide products were identified using electron and x-ray diffraction and the polished cross sections of oxidized alloys were subjected to metallographic and electron microprobe examination.

RESULTS

Oxidation at Linear Heating Rate

Thermograms were obtained for each alloy composition. In Fig. 1 the specific weight gain is plotted against temperature over the range 300 - 1300°C. The plot shows that increasing additions of silicon generally tend to reduce oxidation of nickel. In some cases, however, such as at lower temperatures with silicon additions up to 1%, an increased oxidation is shown. The oxidation behavior becomes complex in the neighborhood of 900°C at or above 3% silicon addition.

For pure nickel, the oxidation curve consists of two parabolic segments joined with a short straight portion around 900 - 1000°C. This suggests two oxidation mechanisms for the temperature ranges below and above 900°C, and coincides with the finding by Berry[5] and Van den Broek[6] who showed a pronounced kink at about 950°C in Arrhenius plots. The oxidation rate of nickel is dependent on the concentration gradient of cation vacancies in the oxide. Vacancy formation at the O/NiO interface is written for nonionized, singly

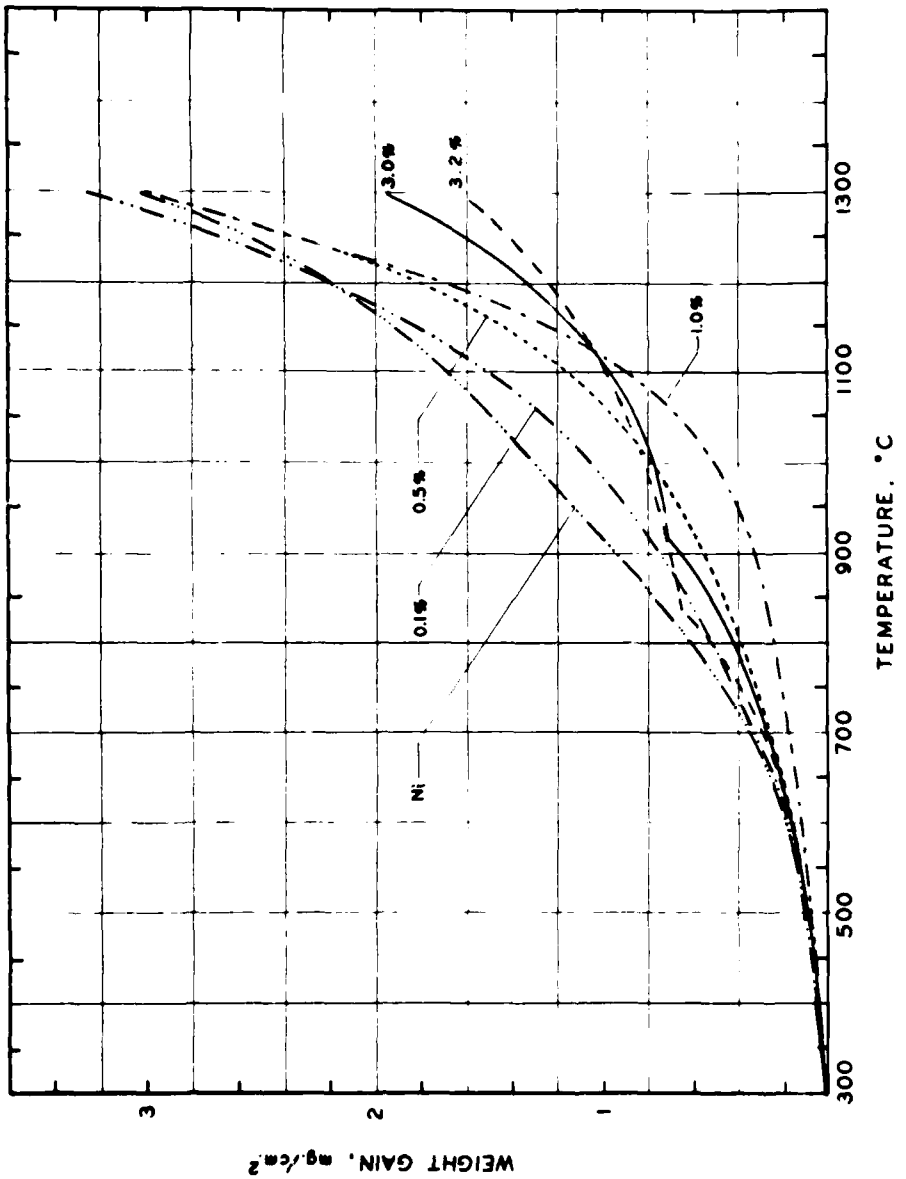

Figure 1. Oxidation of Ni-Si alloys at a linear heating rate in 1 atm. oxygen.

and doubly ionized nickel as follows:

$$1/2\ O_2 \rightleftharpoons V_{Ni} + NiO \qquad (1)$$

$$1/2\ O_2 \rightleftharpoons V'_{Ni} + \oplus + NiO \qquad (2)$$

$$1/2\ O_2 \rightleftharpoons V''_{Ni} + 2\oplus + NiO \qquad (3)$$

Over a limited temperature range, only one charge state for the vacancy is likely to predominate. Berry's data satisfactorily followed the singly ionized nickel vacancy-mechanism(2) at 800 - 900°C and the doubly ionized vacancy mechanism(3) at 1000°C or above. Van den Broek attributed the kink to a change in the number of oxide layers from a single layer at lower temperatures to a double layer at higher temperatures.

For dilute alloys containing up to 1% silicon, oxidation is represented by a single smooth parabolic curve. When the silicon content exceeds 3%, the oxidation is described by two consecutive curves with a break around 900°C and an appreciable reduction in oxidation is observed in the higher temperature region.

Isothermal Oxidation

Oxidation was carried out at three temperatures for 16 hrs. The logarithmic plot of weight gain vs oxidation time is shown in Fig. 2. Most of the data are represented by one or two straight lines indicating the power-law dependence, $(\Delta m)^n = kt$, with n ranging from 1 to 3. In most cases the plots consist of two

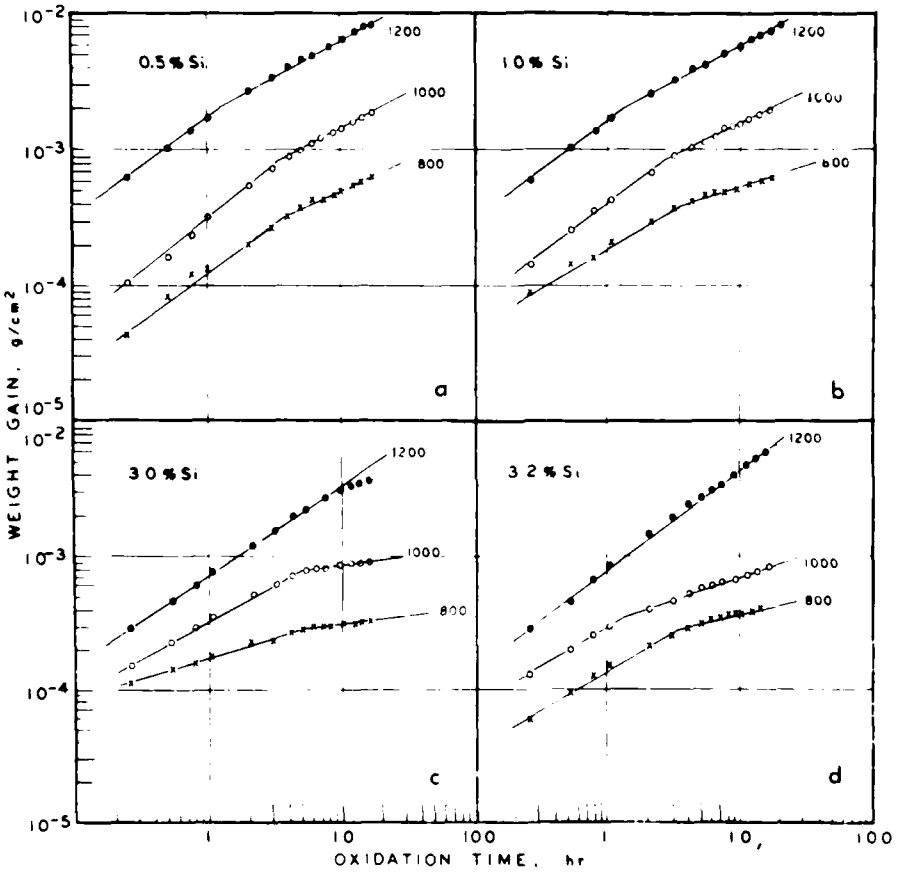

Figure 2. Isothermal oxidation of Ni alloys containing a) 0.5% Si, b) 1.0% Si, c) 3.0% Si and d) 3.2% Si.

straight line portions. For the 0.5 and 1% silicon alloys the plots indicate an initial linear oxidation rate followed by a parabolic rate except for the 1% alloy at 800°C, which is closer to a cubic rate. For the 3% alloy the initial rate changes from cubic (800°C) to parabolic (1000°C) followed by a much higher power rate at longer times. For the 3.2% alloy at 800° and 1000°C the rate changes from the initial parabolic behavior to cubic. At 1200°C both the 3 and 3.2% alloys obey almost a single rate between parabolic and linear.

The oxide formed was analyzed by diffraction techniques. The outer surface of the oxide was identified by electron diffraction. Since the electrons at most penetrate only a few hundred angstroms, this technique shows the oxide present at the outer surface. The electron diffraction data are listed in Table I. All the diffraction patterns showed that the oxide consisted of a single oxide, NiO. In one case (1% Si, heated at 800°C), a small amount of SiO_2 type material was detected in addition to NiO. The oxide was also analyzed by x-ray diffraction which included all of the oxide layer and the base metal. The analyses were performed in a diffractometer using Cu radiation with a nickel filter at 35 KV and 15 milliamperes. Table II lists the diffraction data matching those of NiO and Ni, with the exception of a few where the oxide layer was thick enough to absorb x-rays from the matrix. The oxide scale peeled off from the matrix was analyzed using a powder camera with nickel filtered Cu radiation at 35 KV and 15 milliamperes. Data in Table III indicate a

TABLE I

Electron Diffraction Data - d (Å)

Alloy, % Si	0.5			1.0			3.0			3.2	
Oxid. Temp. (°C)	800	1000	1200	800	1000	1200	800	1000	1200	800	1000
	2.417	2.425	2.419	3.029	2.420	2.410	2.420	2.420	2.416	2.420	2.420
	2.078	2.076	2.073	2.800	2.085	2.072	2.076	2.069	2.066	2.073	2.073
	1.478	1.484	1.489	2.429	1.489	1.485	1.483	1.478	1.469	1.475	1.478
	1.273	1.267	1.266	2.093	1.276	1.272	1.271	1.267	1.255	1.262	1.272
	1.204	1.207	1.206	1.910	1.215	1.213	1.206	1.200	1.210	1.202	1.200
	1.020	1.044	1.043	1.795	1.052	1.048	1.046	1.040	1.026	1.035	1.046
	.959	.960	.958	1.552	.957	.954	.960	.957	.945	.956	.956
	.935	.934	.932	1.493	.867	.867	.930	.933	.853	.934	.930
	.860	.854	.853	1.431	.807		.855	.853		.852	.853
	.813		.804	1.373			.806	.803		.801	.803
				1.280							
				1.215							
				1.154							
				1.078							
				1.050							
				1.010							
				.968							
				.938							
				.850							

TABLE II

X-Ray Diffractometer Data - d (Å)

Alloy, % Si	0.5			1.0			3.0			3.2	
Oxid. Temp. (°C)	800	1000	1200	800	1000	1200	800	1000	1200	800	1000
	2.409	2.409	2.409	2.415	2.415	2.409	2.409	2.409	2.409	2.416	2.415
	2.088	2.088	2.088	2.092	2.090	2.088	2.088	2.088	2.090	2.092	2.088
	2.03	2.030	1.478	2.034	2.037	1.477	2.034	1.478	1.478	2.030	2.033
	1.763	1.760	1.260	1.763	1.760	1.260	1.760	1.261	1.260	1.762	1.757
	1.478	1.478	.959	1.481	1.481	1.207	1.476	1.207	1.207	1.481	1.481
	1.259	1.261	.934	1.261	1.262	1.044	1.260	.959	1.044	1.261	1.275
	1.247	1.244	.853	1.247	1.247	.959	1.246	.935	.935	1.245	1.208
	1.203	1.207		1.207	1.205	.935	1.207	.880	.853	1.207	.959
	1.063	1.045		1.062	1.071	.853	1.063	.878	.804	1.061	.935
	1.044	.960		1.017	1.018		.959	.854		1.016	.854
	1.017	.935		.959	.959		.935			.935	
	.959	.854		.935	.936		.853			.880	
	.935			.850	.882					.853	
	.881				.854						

TABLE III

X-Ray Powder Camera Data - d (Å)

Alloy, % Si	3.2	
Oxid. Temp. (°C)	800	1000
	4.145	4.149
	3.748	3.717
	2.651	3.450
	2.410	2.728
	2.347	2.410
	2.295	2.088
	2.088	1.913
	1.919	1.729
	1.686	1.655
	1.629	1.620
	1.476	1.477
	1.258	1.255
	1.204	1.205

presence of NiO plus a small amount of Ni_2SiO_4. The above findings are summarized in Table IV with those of surface appearance.

Metallographic inspection of the polished cross section of the oxidized alloys revealed a subscale formation of precipitated particles. The outer scale consisted of a mono- or double-layer depending on alloy composition and oxidation temperature. Precipitation of oxide particles followed the general pattern of internal oxidation. Typical photomicrographs are shown in Figs. 3-5. At low temperature precipitation takes place mainly along grain boundaries and with increasing temperature precipitation develops throughout the grain (Fig. 3). With increasing silicon content higher temperatures of oxidation are required for uniformly dispersed precipitate. The 3% silicon alloy showed a little precipitation at lower temperatures, but an evenly dispersed precipitate was observed at 1200°C. (Fig. 4). No appreciable precipitation was observed in the 3.2% alloy (Fig. 5).

To support the above observation, electron microprobe analysis was made for each element while the specimen was traversed at right angles to the original surface for a distance of approximately 200 microns into the metal matrix. The path of the beam is indicated by an arrow in the metallographs. The corresponding traces, shown in Figs. 6-8, indicate the relative distribution of each element. For comparison the representative x-ray images for Ni and Si are shown together with the metallographs in Figs. 3-5. It is readily seen

TABLE IV

Oxidation Product, Appearance & Analysis

% Si	Temperature, °C					
	800		1000		1200	
0.5	gray	NiO (e) NiO+Ni(x)	gray-green	NiO (e) NiO+Ni(x)	met. gray	NiO (e) NiO (x)
1	gray	NiO+tr. SiO_2(e) NiO+Ni(x)	br. gray	NiO (e) NiO+Ni(x)	dark gray	NiO (e) NiO (x)
3	gray	NiO (e) NiO+Ni(x)	gray-green	NiO (e) NiO+Ni(x)	green-d.gray	NiO (e) NiO (x)
3.2	gray-brown	NiO (e) NiO+Ni(x)	gray	NiO (e) NiO+ Ni_2SiO_4(p)	dark gray	NiO+ Ni_2SiO_4(p)

(e) electron diffraction, (x) x-ray diffraction and (p) powder method

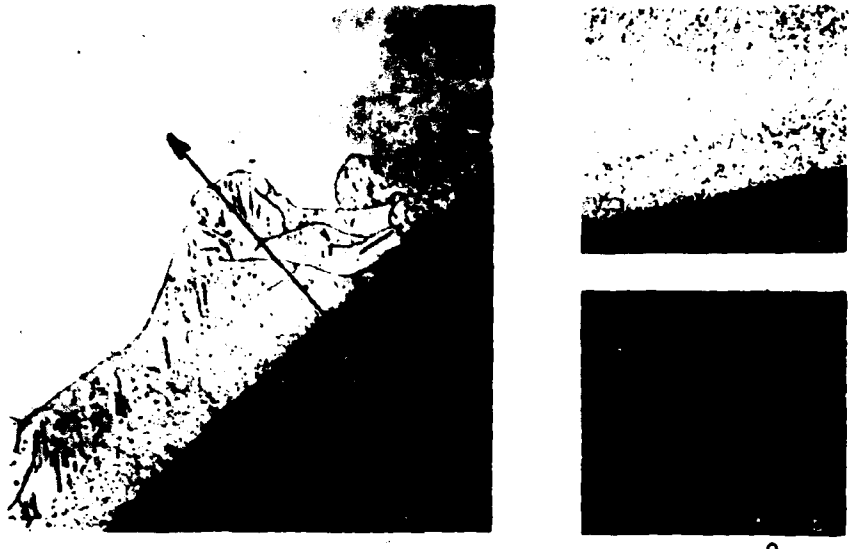

Figure 3. Cross section of Ni - 1.0% Si oxidized at 1200°C for 16 hours, unetched, 250X. a) X-ray image for Ni and b) for Si in the corresponding area.

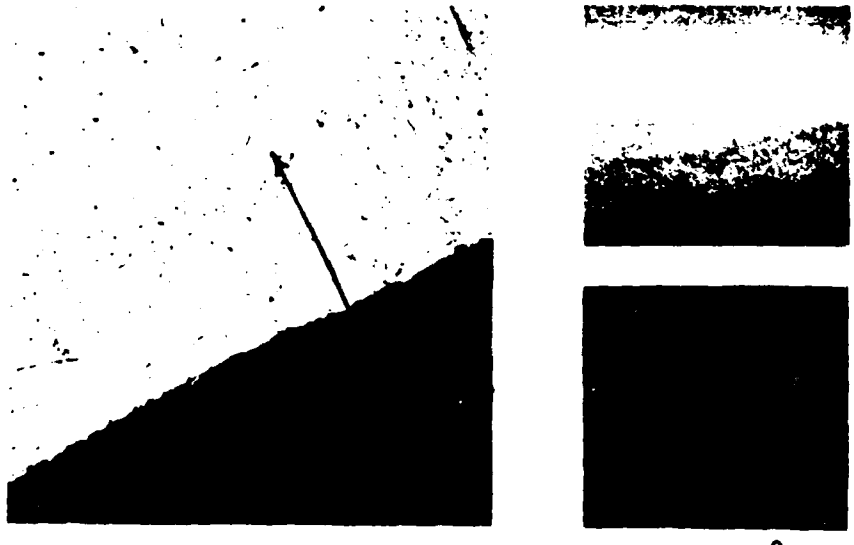

Figure 4. Cross section of Ni - 3.0% Si oxidized at 1200°C for 16 hours, unetched, 250X. a) X-ray image for Ni and b) for Si in the corresponding area.

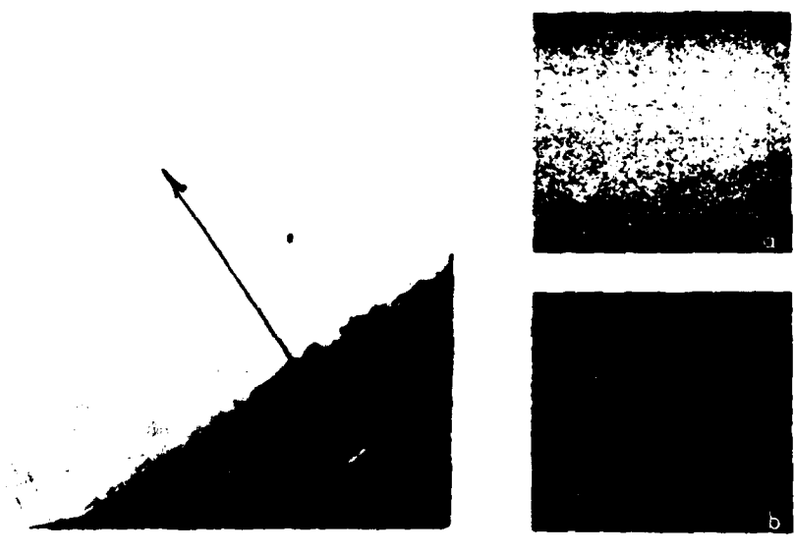

Figure 5. Cross section of Ni - 3.2% Si oxidized at 1200°C for 16 hours, unetched, 250X. a) X-ray image for Ni and b) for Si in the corresponding area.

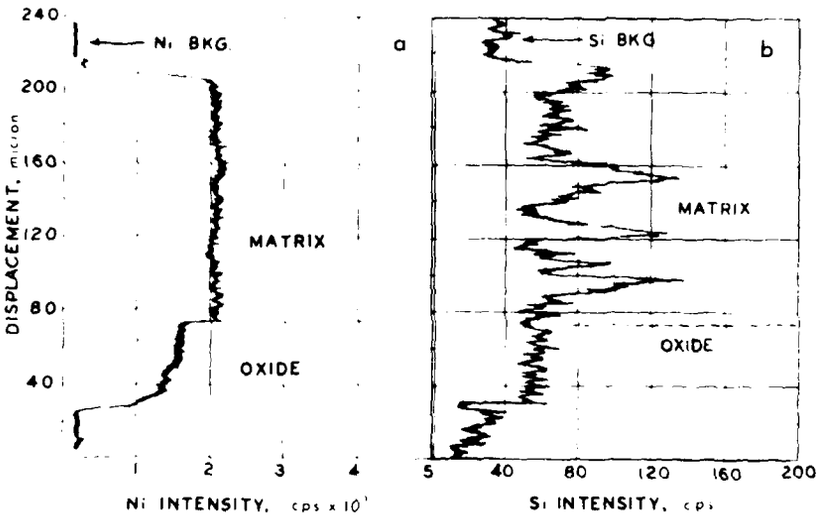

Figure 6. Electron microprobe trace of a) Ni and b) Si on the oxidized Ni - 1.0% Si cross section along an arrow in Figure 3.

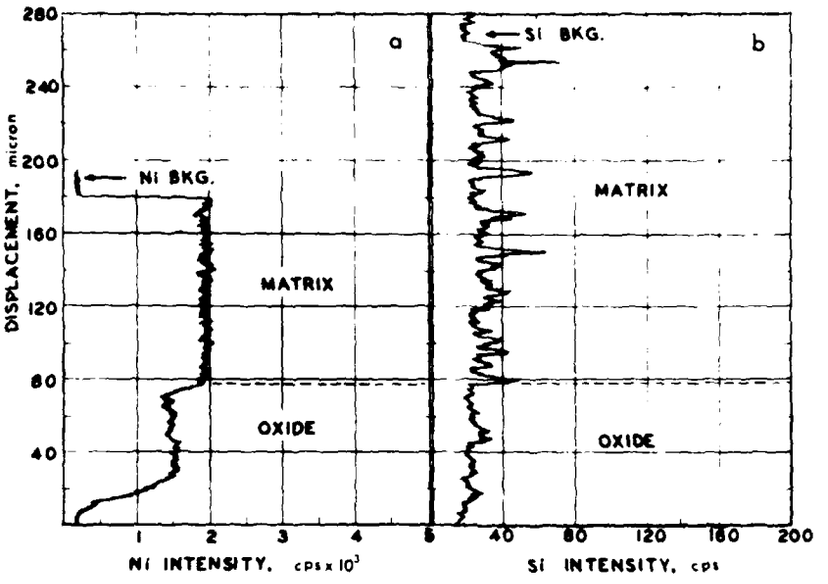

Figure 7. Electron microprobe trace of a) Ni and b) Si on the oxidized Ni - 3.0% Si cross section along an arrow in Figure 4.

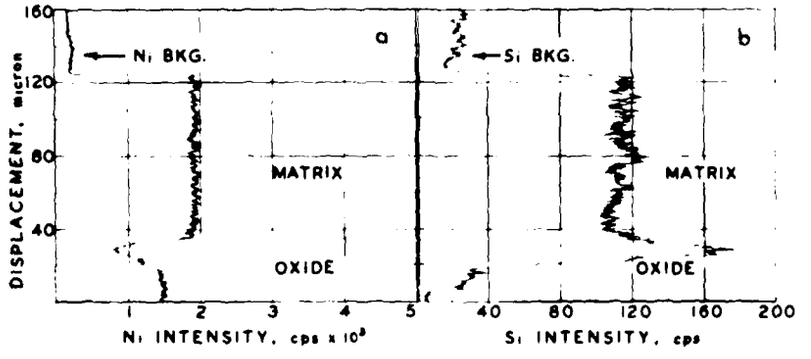

Figure 8. Electron microprobe trace of a) Ni and b) Si on the oxidized Ni - 3.2% Si cross section along an arrow in Figure 5.

that for 1 and 3% alloys no silicon increase is observed in the outer scale. The former shows a broad granular zone adjacent to the scale/metal interface containing a spotty concentration of silicon particularly along grain boundaries. The latter shows small silicon precipitates within a similar area. The 3.2% alloy shows a sharp increase in Si content in the outer layer adjacent to the scale/metal interface and no change in Si within the matrix indicating formation of Ni_2SiO_4 and the absence of internal oxidation.

DISCUSSION

Since thermograms obtained with a linear-heating rate are smooth in the temperature range above 900°C, an activation energy of oxidation can be estimated using Kofstad[7] method.

The general rate law may be expressed by

$$(\Delta m)^{n-1} \frac{d(\Delta m)}{dt} = A \exp \frac{-Q}{RT} \qquad (4)$$

Temperature increase at a linear rate with time is given by

$$T = a t + b \qquad (5)$$

Substituting (5) and A/a = B in (4),

$$(n-1)\ln(\Delta m) + \ln \frac{d(\Delta m)}{dT} = \ln B - \frac{Q}{RT} \qquad (6)$$

The slope of the straight line obtained by a plot of the left side of (6) against 1/T gives an activation energy, Q. Values obtained

in this work (n=2) are listed in Table V. Although this method gives an approximate value, the data indicate a marked difference from that of nickel metal. The values obtained in this work for nickel were in agreement with those of Berry and Van den Broek, who gave 24 and 20 kcal/mole for the temperature range below 950°C, and 57 and 50 kcal/mole above 950°C, respectively.

Since NiO is a metal deficit, p-type semiconductor the oxidation of nickel is controlled by diffusion of nickel ions through cation vacancies and electron holes. Recently Mrowec[8] explained the double layer formation mechanism by outward diffusion of cation in two stages: (1) a compact monolayer scale is formed until the consumption of metal is compensated by the plastic flow of the scale, and (2) at a certain critical thickness the scale begins to lose its contact with metal by crack development. Consequent reduction in the rate of metal transport leads to secondary formation of a porous layer followed by gradual dissociation of the outer layer. The morphological structure depends on the plastic deformation of the reaction product, surface geometry, and reaction time and temperature.

In Ni-Si alloys the base metal oxide, NiO, is formed principally by the outward diffusion of nickel ions through the scale whereas internal oxidation takes place by the inward transport of oxygen to form SiO_2 precipitates in the matrix. The internally

TABLE V

Activation Energy, Q (Kcal/mole)

Ni		Ni - Si alloys (% Si)			
500-800°C	950-1300°C	0.1%	0.5%	1%	3.0%
20.8	46.5	60.2	59.7	61.3	65.0

formed SiO_2 can further react with NiO at the scale/metal interface to form a silicate. The total reaction is written as follows with free energy changes at 1000°C:

$$Ni(s) + 1/2\ O_2(g) = NiO(s): \quad \Delta G_7^\circ = -35{,}900 \text{ cal} \qquad (7)^9$$

$$Si(s) + O_2(g) = SiO_2(s): \quad \Delta G_8^\circ = -166{,}800 \text{ cal} \qquad (8)^9$$

$$2NiO + SiO_2 = Ni_2SiO_4(s): \quad \Delta G_9^\circ = -7{,}340 \text{ cal} \qquad (9)^{10}$$

It was observed that a small addition of Si increased the oxidation of nickel in some cases. The introduction of Si^{+4} to the NiO lattice requires dissolution of internally oxidized SiO_2 at the NiO/Ni interface. The amount of Si in equilibrium at the interface in solid solution in Ni can be calculated by the following equilibrium constant:

$$SiO_2(s) \longrightarrow \underline{Si}\ (\text{alloy}) + O_2(g) \qquad (10)$$

$$RT \ln K_{10} = RT \ln a_{Si}\ Po_2 = \Delta G_8^\circ \qquad (11)$$

Using values for ΔG_8° and $Po_2 = 5.0 \times 10^{-11}$ atm (NiO/Ni) at 1000°C, (11) yields $a_{Si} = 2.0 \times 10^{-16}$ (1000°C). It can also be seen that a very slight amount of silicon is needed to initiate internal oxidation.

When a small amount of Si is added to nickel, the oxide precipitation taking place at the scale/metal interface in the initial stage of reaction gives rise to break down of full contact

between scale and metal. Thus the stage(2) described in the case of pure nickel takes place immediately at the interface resulting in formation of a porous inner layer and loss of compactness of the outer layer, which is growing by outward diffusion of nickel ion. If the anisotropic dissociation of the outer layer or the transport of oxygen in the crack is the slow process, the formation of the inner porous layer follows a linear rate law. With increasing thickness of the porous inner layer, diffusion becomes a rate-determining step. The oxidation kinetics, therefore, are characterized by a shift from linear to parabolic at a certain thickness of the porous layer as shown in 0.5 and 1.0 alloys (Fig. 2, a b).

Generally plastic flow of the scale is not observed in the binary alloys, and the inward transport of oxygen molecules is carried out through perpendicular discontinuities in the scale while the outer layer is formed by outward lattice diffusion of metal. In the 3% alloy oxidation kinetics are controlled by parabolic diffusion until the internal oxide precipitate becomes a mechanical obstacle to the diffusion process (Fig. 2, c). In the 3.2% alloy, where no internal oxidation is observed, the initial reaction kinetics are parabolic diffusion controlled (Fig. 2, d).

The quasi-cubic rate observed at 800°C for the 1 and 3% alloys appears to be caused by a superposition of two parabolic steps, whereby the rate constant of gas consumption becomes

smaller as time increases[11]. At higher temperatures where the scale loses its adherence to the metal, the parabolic rate tends to deviate towards a linear rate.

The secondary solid-solid reaction between the oxides are observed only at the 3.2% alloy. To calculate the silicon content at which an alloy is in thermodynamic equilibrium with a mixture of Ni_2SiO_4 and SiO_2, the following equation is written

$$Ni_2SiO_4(s) + Si\ (alloy) = 2\ SiO_2(s) + 2\ Ni\ (alloy) \qquad (12)$$

The equilibrium constant is

$$RT \ln K_{12} = RT \ln a_{Ni}^2/a_{si} = - \Delta G^\circ_{12}$$

where

$$\Delta G^\circ_{12} = \Delta G^\circ_8 - 2\ \Delta G^\circ_7 - \Delta G^\circ_9 = -87{,}660 \text{ cal } (1000^\circ C)$$

Thus for $a_{Ni} = 1$, $a_{Si} = 1.1 \times 10^{-15}$. It appears that SiO_2 is more stable at the scale/metal interface, if the silicon content does not fall below this value. The formation of Ni_2SiO_4 phase, however, has no effect on the weight change measurements.

Recently a mathematical treatment on the growth rate of sub-scale depth on simultaneous external and internal oxidation was developed by Maak[12] extending Wagner's equation. However, further information on precipitation dispersion is awaited for application of this treatment to thermogravimetry.

CONCLUSIONS

The addition of silicon generally increased the oxidation resistance of nickel. In most cases, isothermal oxidation followed two consecutive power-law relationships in different reaction orders depending on temperature and alloy composition. With increasing silicon more than 3%, the oxidation thermogram of Ni-Si alloys exhibited two distinct consecutive curves diverging at about 900°C.

The scale NiO consisted of a single oxide NiO and a subscale of SiO_2 precipitate caused by a simultaneous internal oxidation. For the 3.2% Si alloy, Ni_2SiO_4 was detected in NiO scale without internal oxidation.

REFERENCES

1. B. E. Deal and A. S. Grove, J. Appl. Phys. 36, 3770 (1965).

2. A. G. Revesz, K. H. Zaininger and R. J. Evans, Appl. Phys. Letters 8, 57 (1966).

3. L. Horn, Z. Metallk. 40, 73 (1949).

4. I. S. Gil'dengorn and I. L. Rogel'berg, Fiz. Metal. Metalloved. 17, 527 (1964).

5. L. Berry and J. Paidassi, Compt. Rend. 262C, 1353 (1966).

6. J. J. Van den Broek and J. L. Meijering, Acta Met. 16, 375 (1968).

7. P. Kofstad, Nature Lond. 179, 1362 (1957).

8. S. Mrowec, Corros. Sci. 7, 563 (1967).

9. J. F. Elliott and M. Gleiser, "Thermochemistry for Steelmaking", Vol. 1 (1960).

10. N. A. Toropov and V. P. Bazakovskii, "High-Temperature Chemistry of Silicates and Other Oxide Systems", Transl., Consultant Bur., New York (1966).

11. K. Hauffe, "Oxidation of Metals", Plenum Press, N. Y. (1965).

12. F. Maak, Z. Metallk. 52, 545 (1961).

Unclassified

Security Classification

DOCUMENT CONTROL DATA - R & D

(Security classification of title, body of abstract and indexing annotation must be entered when the overall report is classified)

1 ORIGINATING ACTIVITY *(Corporate author)*
Watervliet Arsenal
Watervliet, New York 12189

2a. REPORT SECURITY CLASSIFICATION
Unclassified

2b. GROUP

3 REPORT TITLE
THE OXIDATION MECHANISM OF NICKEL SILICON ALLOY

4 DESCRIPTIVE NOTES *(Type of report and inclusive dates)*
Technical Report

5 AUTHOR(S) *(First name, middle initial, last name)*
FUMIHIKO SAEGUSA

6. REPORT DATE	7a. TOTAL NO. OF PAGES	7b. NO. OF REFS
December 1968	34	12

8a. CONTRACT OR GRANT NO.
AMCMS No. 5025.11.29400

b. PROJECT NO
DA Project No. 1-C-0-24401-A328

c.

d.

9a. ORIGINATOR'S REPORT NUMBER(S)
WVT-6837

9b. OTHER REPORT NO(S) *(Any other numbers that may be assigned this report)*

10 DISTRIBUTION STATEMENT
This document has been approved for public release and sale; its distribution is unlimited.

11 SUPPLEMENTARY NOTES

12. SPONSORING MILITARY ACTIVITY
U. S. Army Weapons Command

13 ABSTRACT

Thermogravimetric techniques have been used to study oxidation of nickel alloys containing 0.1 to 3.2 wt % silicon at temperatures up to 1300°C. Due to the appearance of internal oxidation the effect of silicon addition on the oxidation process was complex. The thermograms showed a simple curve for lower silicon content, but two consecutive curves for higher content. The oxidation mechanism was interpreted in terms of isothermal kinetics and the corresponding structural changes.

DD FORM 1 NOV 68 1473 REPLACES DD FORM 1473, 1 JAN 64, WHICH IS OBSOLETE FOR ARMY USE.

Unclassified

Security Classification

14. KEY WORDS	LINK A		LINK B		LINK C	
	ROLE	WT	ROLE	WT	ROLE	WT
Oxidation						
Corrosion						
Nickel						
Silicon						
Nickel alloys						